0026-895X/11/7905-844–854$25.00
MOLECULAR PHARMACOLOGY
Vol. 79, No. 5
69831/3683782
Mol Pharmacol 79:844–854, 2011
Printed in U.S.A.

Early Failure of *N*-Methyl-D-aspartate Receptors and Deficient Spine Formation Induced by Reduction of Regulatory Heme in Neurons[S]

Tatyana Chernova, Joern R. Steinert, Paul Richards, Rajendra Mistry, R. A. John Challiss, Rebekah Jukes-Jones, Kelvin Cain, Andrew G. Smith, and Ian D. Forsythe

MRC Toxicology Unit, University of Leicester, Leicester, United Kingdom (T.C., J.R.S., P.R., A.G.S., R.J.-J., K.C., I.D.F.); and Department of Cell Physiology and Pharmacology (R.M., R.A.J.C.), University of Leicester, Leicester, United Kingdom

Received November 9, 2010; accepted February 15, 2011

ABSTRACT

An initial stage of many neurodegenerative processes is associated with compromised synaptic function and precedes synapse loss, neurite fragmentation, and neuronal death. We showed previously that deficiency of heme, regulating many proteins of pharmacological importance, causes neurodegeneration of primary cortical neurons via *N*-methyl-D-aspartate receptor (NMDAR)-dependent suppression of the extracellular signal-regulated kinase 1/2 pathway. Here, we asked whether the reduction of heme causes synaptic perturbation before neurite fragmentation in neuronal cultures and investigated molecular mechanisms of synaptic dysfunction in these cells. We showed the change in the NR2B subunit phosphorylation that correlates with compromised NMDAR function after the reduction of regulatory heme and a rapid rescue of NR2B phosphorylation and NMDAR function by exogenous heme. Electrophysiological recordings demonstrated diminished NMDAR currents and NMDAR-mediated calcium influx after 24 h of inhibition of heme synthesis. These effects were reversed by treatment with heme; however, inhibition of the Src family kinases abolished the rescue effect of heme on NMDA-evoked currents. Diminished NMDAR current and Ca^{2+} influx resulted in suppressed cGMP production and impairment of spine formation. Exogenous heme exerted rescue effects on NR2B tyrosine phosphorylation and NMDA-evoked currents within minutes, suggesting direct interactions within the NMDAR complex. These synaptic changes after inhibition of heme synthesis occurred at this stage without apparent dysfunction of major hemoproteins. We conclude that regulatory heme is necessary in maintaining NR2B phosphorylation and NMDAR function. NMDAR failure occurs before neurite fragmentation and may be a causal factor in neurodegeneration; this could suggest a route for an early pharmacological intervention.

Introduction

Neurodegeneration progresses from reversible down-regulation of synaptic function to irreversible synapse loss and neuronal death, so rescue at such an early stage of synaptic loss offers an attractive approach for therapeutic intervention (Wishart et al., 2006; Mallucci, 2009). Elucidating mechanisms causing neurodegenerative process requires capturing an earlier synaptic perturbation, which is not always easy in existing in vivo and in vitro models of neurodegeneration (Boekhoorn et al., 2006; Soto and Estrada, 2008). Here, we focus on early stages of synaptic dysfunction before neurite fragmentation in primary neurons with reduced level of heme and on identifying factors triggering synaptic loss that has greater potential to facilitate pharmacological strategies to reverse neurodegeneration.

Deficiency of heme is detrimental to neurons and is a contributory factor in cell aging (Chernova et al., 2006), Alzheimer's disease (Atamna and Frey, 2004), and drug-induced neurotoxicity (Meyer et al., 2005). It also diminishes neuron-specific gene expression, alters cellular signaling, and induces apoptosis (Zhu et al., 2002). Heme synthesis is up-regulated during the differentiation of cultured neuronal cells (Shinjyo and Kita, 2006) and exogenous heme promotes outgrowth of neurites (Ishii and Maniatis, 1978). Heme exists in at least two pools in cells: heme bound within hemoproteins, and "free" heme (i.e., not associated with a protein).

Article, publication date, and citation information can be found at http://molpharm.aspetjournals.org.
doi:10.1124/mol.110.069831.
[S] The online version of this article (available at http://molpharm.aspetjournals.org) contains supplemental material.

ABBREVIATIONS: NMDAR, *N*-methyl-D-aspartate receptor; ALAS, aminolevulinic acid synthase; nNOS, neuronal nitric-oxide synthase; SFK, Src family kinase; PP2, 4-amino-5-(4-chlorophenyl)-7-(*t*-butyl)pyrazolo[3,4-*d*]pyrimidine; SA, succinyl acetone; PCR, polymerase chain reaction; DIV, days in vitro; aCSF, artificial cerebrospinal fluid; BSA, bovine serum albumin; PSD, postsynaptic density; sGC, soluble guanylate cyclase; HO-1, heme-oxygenase-1.

A portion of the unbound heme forms a regulatory pool that mediates a signaling role through binding to heme-regulatory motifs in proteins and modulating their functions; this includes ion channels (Tang et al., 2003), transcription factors (Ogawa et al., 2001), and nuclear receptors (Raghuram et al., 2007). We demonstrated previously that heme is necessary to maintain neurite integrity, whereas heme deficiency causes neurodegeneration via NMDA receptor (NMDAR)-dependent suppression of the extracellular signal-regulated kinase 1/2 pathway. Heme-deficient cultured neurons displayed progressive neurite fragmentation followed, eventually, by cell death. The rescue of prosurvival extracellular signal-regulated kinase 1/2 activation by heme was mediated predominantly via the NR2B-containing NMDARs (Chernova et al., 2007). These observations were made in neurons chronically deficient in heme, in which the loss of both bound and regulatory heme pools might have contributed to the progressive fragmentation of neurites.

Here, we tested the hypothesis that heme is necessary for the regulation of NMDAR and that a lack of "free" heme rapidly causes this ion channel dysfunction. We have examined the early stage of heme deficiency in cortical cultures and identified an early NMDAR impairment. Failure of NMDAR function occurred shortly (16–24 h) after reduction of regulatory heme and was reflected by markedly decreased NMDAR currents and Ca^{2+} influx. This correlated with a reduction in the phosphorylation of the NR2B subunit of NMDARs. In addition, NMDAR-dependent cGMP production was compromised, and dendritic spine formation reduced. Exogenous heme rescued the ion channel function and spine formation, but only if normal levels of NR2B phosphorylation were resumed. We have demonstrated that heme modulates NMDAR function and tyrosine phosphorylation of NR2B subunit within minutes in a signaling mode and requires Src family kinases (SFKs) activity. Heme bound to major hemoproteins was preserved and the functions of tested proteins were unaffected. These findings suggest that early synaptic impairment after inhibition of heme synthesis is caused by the reduction of regulatory heme. We conclude that NMDAR failure occurs before neurite fragmentation at the early stage of heme deficiency and may be a causal factor in neurodegeneration.

Materials and Methods

Primary Cell Culture. Primary cortical neurons were prepared from either male or female 14-day-old fetuses of the BALB/c mouse strain bred in-house. The isolated neocortex of embryos was gently dissociated to release the neurons, which were washed twice in Neurobasal medium (Invitrogen, Carlsbad, CA) supplemented with 10% fetal calf serum. Cell suspensions were plated on poly(L-lysine)-coated 35-mm plates at a density of 10^6 cells/dish. After attachment of the cells, the plating medium was changed to serum-free culture medium containing 96% (v/v) Neurobasal medium (Invitrogen), 2 μM GlutaMAX, 2% B-27 supplement (Invitrogen, Paisley, UK), 100 μg/ml streptomycin, and 100 U/ml penicillin. Viability of the cells was estimated by the trypan blue exclusion assay and typically was approximately 85%. After 5 days, 10 μM cytosine arabinoside (1β-arabinofuranosylcytosine) was added to the culture medium for 3 days to stop proliferation of glial cells or fibroblasts. The cells were grown in a humidified incubator at 37°C (95% room air/5% CO_2). Selective inhibitor of SFKs 4-amino-5-(4-chlorophenyl)-7-(*t*-butyl)pyrazolo[3,4-*d*]pyrimidine (PP2) (Calbiochem, San Diego, CA) was applied at 50 nM for 24 h to control cells and to the treated cell treated with succinyl acetone (SA) ± heme, or for 2 h in 2-h heme readmission after SA treatment.

Inhibition and Readmission of Heme, Measurement of Cellular Heme Content, and Heme Synthesis. To inhibit heme synthesis, cells were cultured in serum-free medium with 250 μM SA (4,6-dioxoheptanoic acid) (Sigma-Aldrich, Dorset, UK) for the stated durations. For heme readmission experiments, cells were treated daily with 100 nM hemin (iron protoporphyrin IX); stock solution was added to human serum albumin in a 1:1 M ratio before treatment. The heme concentrations were verified spectrophotometrically.

Total cellular heme was measured by using a modified QuantiChrom Heme Assay (BioAssay Systems, Hayward, CA). The optical density measurements were taken using NanoDrop 2000 Spectrophotometer (Thermo Fisher Scientific, Waltham, MA). The amount of heme in each sample was expressed as micromoles of heme per milligram of total protein. For measurement of heme synthesis, cells were incubated with 0.4 μCi of [3,5-^{3}H]aminolevulinic acid hydrochloride (2.6 Ci/mmol; PerkinElmer Life and Analytical Sciences, Waltham, MA) for 24 h. Heme was extracted from the cells by acetone-HCl and diethyl ether. The amount of radioactivity in extracted heme was measured by scintillation counting as described previously (Chernova et al., 2007). Total recovery of radioactivity from all fractions was the same for treated and untreated cells.

RNA Extraction and Quantitative Real-Time PCR Analysis. Total RNA was isolated from treated and untreated cells at different time points by using TRI reagent (Sigma-Aldrich), and cDNA synthesis was performed using random primers and Superscript II (Invitrogen, Carlsbad, CA). PCR primers were selected using the Primer Express version 2.0 Software program (Applied Biosystems, Foster City, CA). Primers sequences were as follows: β-actin forward primer, 5′-GATTACTGCTCTGGCTCCTAGCA-3′, reverse primer, 5′-GTGGACAGTGAGGCCAGGAT-3′; δ-aminolevulinate synthase 1 (*ALAS1*) forward primer, 5′-TCTTC-CGCAAGGCCAGTCT-3′, reverse primer, 5′-TGGGCTTGAGCAGCCTCTT-3′; and *CYP4X1* forward primer, 5′-CCTGGACATAATAATGAAATGTGCTT-3′, reverse primer, 5′-CTTCACGTAAGACTCATAGGTGCC-3′.

Primers were designed to cross exon-exon boundaries. PCR was performed using SYBR Green PCR Master Mix, primers, and 10 ng of reverse-transcribed cDNA in the ABI Prism 7700 Sequence Detection System (Applied Biosystems) as described previously (Kannan et al., 2010). Quantification was performed using the comparative CT method (ΔΔCT). Data are presented as the mean ± S.D. (n = 3–8 for each group). Statistical significance was assessed as $p < 0.05$ using one-way analysis of variance.

Immunocytochemistry. After treatment, cells were fixed with 4% paraformaldehyde at room temperature for 20 min and permeabilized with 0.2% Triton X-100 (Sigma-Aldrich) in phosphate-buffered saline for 5 min. Cells were then incubated with rabbit anti-phospo-NR2B (Tyr1252 or Tyr1336) (R&D Systems, Abingdon, UK) and mouse anti-PSD-95 antibody (NeuroMab, Davis, CA) at room temperature for 1 h. Secondary antibodies (goat anti-rabbit Alexa Fluor 546 and goat anti-mouse Alexa Fluor 488 at 1:500) were then added for 1 h, followed by nuclear staining with 300 nM 4′-6-diamidino-2-phenylindole for 10 min. Secondary antibodies alone were used as specificity controls and uniformly resulted in very low background levels of fluorescence.

Transfection of Cortical Neurons. At 7 DIV, neurons were transfected with plasmids expressing FLAG-tagged tdTomato as a cell fill provided by Dr. Michael J. Schell (Department of Pharmacology, Uniformed Services University, Bethesda, MD) to visualize dendritic morphology. A total of 0.5 μg of DNA and 1 μl of Lipofectamine 2000 (Invitrogen) was premixed according to the manufacturer's instructions and added to cultures (0.5×10^6 cells) growing on glass-bottomed chambers (Thermo Fisher Scientific) in 900 μl of medium. After 6 h, the medium was replaced with a fresh 900 μl of serum-free Neurobasal medium supplemented as described above.

Transfection efficiency was estimated to be less than 2%. Neurons were imaged at 13 DIV.

Imaging and Quantification of Spines. Cortical neurons with pyramidal morphology were selected for analysis from the transfected cell population. Images of cultured cells were obtained with a Zeiss LSM 510 META confocal microscope equipped with a 63× oil immersion lens (Carl Zeiss, Thornwood, NJ). Images were collected as a series of Z-sections (approximately 0.5 μm). Images were reconstructed using Volocity software (Improvision, Coventry, UK). Total protrusions from the dendrite (spines) were quantified over unit length and expressed as the number per 10 μm of the neurites. Only fields with a low density of transfected neurons were used to quantify the spine length and number.

Immunoblotting. Proteins were extracted from primary neurons using NP-40 lysis buffer (1% NP-40, 20 mM Tris-HCl, pH 8.0, 137 mM NaCl, 10% glycerol, 2 mM EDTA, 1 mM sodium orthovanadate, 10 μg/μl leupeptin, and 10 μg/μl aprotinin) and brief sonication. Microsomal fraction was prepared as described previously (Kapoor et al., 2006). In brief, the cells were scraped in phosphate-buffered saline and then pelleted by centrifuging at 200*g* for 10 min. The cell pellet was resuspended in microsomal dilution buffer containing 0.1 (v/v) glycerol, 0.25 mM phenylmethylsulfonyl fluoride, 0.01 M EDTA, and 0.1 mM dithiothreitol. After brief sonication, the cells were centrifuged at 9000*g* for 20 min. The supernatant was then further centrifuged at 105,000*g* for 60 min to isolate the microsomes. The microsomal pellet was resuspended in microsomal dilution buffer and used for analysis. Separation by SDS-polyacrylamide gel electrophoresis or native polyacrylamide gel electrophoresis [for neuronal nitric-oxide synthase (nNOS) detection] was followed by immunoblotting and enhanced chemiluminescence detection (GE Healthcare, Chalfont St. Giles, Buckinghamshire, UK). Antibodies were from the following sources: NMDAR NR1 and total NR2B were from Santa Cruz Biotechnology (Santa Cruz, CA); NMDAR phospho-NR2B Tyr1252 and Tyr1336 were from R&D Systems; α-tubulin was from Sigma-Aldrich; ALAS1 was from Abcam plc (Cambridge, UK), heme-oxygenase-1 (HO-1) and P450 reductase antibodies were from AKELA Pharma Inc. (Montreal, QC, Canada), CYP1A1 was from Cambridge Bioscience (Cambridge, UK) and CYP4X1 was from Dr. D. Bell (School of Biology, University of Nottingham, Nottingham, UK). Blots were subsequently exposed to a second primary antibody against α-tubulin, to verify equivalent protein loading and transfer. Bands were detected by enhanced chemiluminescence (GE Healthcare), exposed to X-ray films under nonsaturating conditions. Results were quantified using densitometry and ImageQuant 5.2 software (GE Healthcare). All comparisons were made within blots. Statistical significance was estimated using two-tailed Student's *t* test.

NMDA Application. Agonist application experiments on primary cortical cultures were performed using a Picospritzer III (Intracel, Frederick, MD) connected to a patch electrode filled with artificial cerebrospinal fluid (aCSF) containing 100 μM NMDA (Sigma-Aldrich). The tip of the electrode was placed near a patch-clamped cortical neuron, and the maximal response to the agonist was optimized by adjusting the pipette position. Puffs were applied for 30 ms every 8 s (20 psi) in the presence of 6,7-dinitroquinoxaline-2,3-dione (10 μM), D-serine (10 μM), and bicuculline (10 μM). No extracellular Mg^{2+} was added to these solutions. To create a current-voltage (I–V) relationship for NMDA-evoked currents, we applied NMDA while holding at different potentials ranging from −60 to +40 mV.

Electrophysiology. Whole-cell patch-clamp recordings were made from primary cultures of cortical neurons [visualized at 60× with a Nikon E600FN (Nikon, Tokyo, Japan) fitted with differential interference contrast optics] using a multiclamp 700B amplifier and pClamp 9 software (both from Molecular Devices, Sunnyvale, CA). Data were sampled at 50 kHz and filtered at 10 kHz. Patch pipettes were pulled from borosilicate glass capillaries (Harvard Apparatus, Edenbridge, UK) using a two-stage vertical puller (Narishige, Tokyo, Japan). Tips were polished (Micro Forge; Narishige), and pipettes had a final open-tip resistance of ~5 MΩ when filled with a patch solution containing the following: 130 mM CsCl, 10 mM HEPES, 5 mM EGTA, and 1 mM $MgCl_2$, pH adjusted to 7.2 with CsOH. Whole-cell access resistances were <20 MΩ. Bath solution was without extracellular $[Mg^{2+}]$ and as follows: 135 mM NaCl, 3 mM KCl, 10 mM HEPES, 2 mM $CaCl_2$, 10 mM glucose, and 45 mM sucrose. Where specified, heme was added to the bath solution or directly to the pipette solution at 0.1 μM.

Ca^{2+} Imaging. For $[Ca^{2+}]_i$ determinations, subconfluent cortical neurons were cultured on glass coverslips and loaded for 10 min at room temperature with 5 μM Fura 2-AM (Invitrogen) aCSF. After loading, cells were kept in aCSF for up to 1 h. Fluorescence was measured using a computer-controlled Polychrome II Monochromator (TILL Photonics, Martinsried, Germany) with excitation at 340, 360, and 380 nm and emission detected at >505 nm. The ratio of fluorescence at 340 and 380 nm excitation was used as a measure of $[Ca^{2+}]_i$. Fluorescence was detected using a charge-coupled device PentaMAX camera (Princeton Instruments, Trenton, NJ). Data were recorded and analyzed using Meta Imaging (series 7.0) software (Molecular Devices). A pair of images was obtained every second with 20-ms exposure time at each wavelength. Fluorescence measurements were preformed in the cell soma. Only cells with low resting ratios (<0.6) and cells that returned to basal ratios after stimulation were used for analysis.

Radioimmunoassay of cGMP. Control, NO-donor *S*-nitroso-*N*-acetylpenicillamine (Sigma-Aldrich)-stimulated or NMDA-stimulated (10 min, 100 and 50 μM, respectively) cortical cultures were used for assessing cGMP production. In brief, neutralized cell extracts were diluted 5-fold in 100 mM sodium acetate, pH 6.2, and acetylated by consecutive addition of triethylamine (10 μl) and acetic anhydride (5 μl) and used in the radioimmunoassay (Brooker et al., 1979) within 60 min. cGMP standards (100 μl; 0–4 nM) were treated identically. Acetylated samples (100 μl) were mixed with 2′-*O*-succinyl [3-^{125}I]iodotyrosine methyl ester cGMP (GE Healthcare) [50 μl, ~3000 d.p.m. made up in 50 mM sodium acetate, 0.2% bovine serum albumin (BSA), pH 6.2] and 100 μl of anticyclic GMP antibody (GE Healthcare; diluted in 50 mM sodium acetate and 0.2% BSA, pH 6.2). Samples were intermittently vortex-mixed during a 4-h incubation at 4°C. Free and bound cGMP was separated by charcoal precipitation with 500 μl of a charcoal suspension [1% (w/v) activated charcoal in 100 mM potassium phosphate, 0.2% BSA, pH 6.2]. After vortex-mixing for 5 min, samples were centrifuged (13,000*g*, 4 min, 4°C), and radioactivity was determined in an aliquot of supernatant (600 μl). Unknown values were determined from the cGMP standard curve using GraphPad Prism 4 (GraphPad Software Inc., San Diego, CA).

Detection of Mitochondrial Membrane Potential. Mitochondrial membrane potential ($\Delta\Psi$m) was detected using DePsipher Kit for Detection of Mitochondrial Membrane Potential Disruption (R&D Systems) according to the manufacturer's instructions. Lipophilic cationic dye 5,5′,6,6′-tetrachloro-1,1′,3,3′-tetraethylbenzimidazoyl carbocyanine iodide enters the inner mitochondrial matrix in its monomeric form when the mitochondrial membrane is polarized. When the mitochondrion has a high $\Delta\Psi$m, the dye crosses the membrane and forms aggregates, which appear red under UV light. Living neurons were stained and observed immediately with a microscope using a long-pass filter (fluorescein and rhodamine). In healthy cells, the mitochondria were stained red after aggregation of the DePsipher within the mitochondria. In cells with disrupted $\Delta\Psi$m, the dye remains in its monomeric form in the cytoplasm and appears entirely green.

Measurement of ATP in Neurons. Cultured neurons were treated with 250 μM SA for 1 to 6 days and harvested at 12 DIV. The level of cellular ATP in neurons was determined with a luciferase-based CellTiter-Glo Luminescent Cell Viability Assay (Promega, Madison, WI) according to the manufacturer's recommendations. After the plates were developed, luminescence was measured in a microplate luminometer (Luminoskan; Labsystems, Helsinki, Fin-

land). Each set of data was collected from multiple replicate wells of each experimental group from five independent experiments; the concentrations were normalized against total cellular protein and expressed as nanomoles per milligram of protein (mean± S.D.).

Results

Inhibition of Heme Synthesis Promptly Reduced Regulatory Pool of Intracellular Heme. To examine the chronology of the neuronal deficit with reduced heme, we inhibited its synthesis for 1 to 6 days by treatment with 250 μM SA, a specific inhibitor of aminolevulinic acid dehydratase (Sassa and Nagai, 1996). Heme synthesis was reduced by approximately 50% (Fig. 1A), causing 17 ± 6% decrease of total intracellular heme (Fig. 1B). This reduction was accompanied by a marked increase in the expression of *ALAS1* (Fig. 1C), the gene encoding aminolevulinic acid synthase, which is under negative transcriptional feedback control by the regulatory pool of intracellular heme (Sassa and Nagai, 1996; Sassa, 2004). The up-regulation of *ALAS1* expression in SA-treated neurons indicated that the decrease in heme was physiologically significant, and this was a rapid process, occurring within hours after inhibition of synthesis. After 16 h of SA treatment *ALAS1* mRNA increased 2-fold, similar to the up-regulation observed in continuously deficient neurons (Chernova et al., 2006). An increased amount of ALAS1 protein in response to reduced heme levels was detected in these SA-treated cultures (Fig. 1D), consistent with previously shown regulation by "free" heme via alterations in protein half-lives (Zheng et al., 2008). By contrast, when heme was added back to SA-treated cells, there was a 24 ± 2% increase in intracellular heme, accompanied by a decrease in *ALAS1* expression, again consistent with a regulated physiological response (Fig. 1, B and C). Our results suggest that the regulatory pool of heme was compromised within hours if de novo synthesis was inadequate. We examined how a lack of regulatory heme affected neuronal function and tested whether NMDAR was compromised in neurons with reduced regulatory heme. We chose a 24-h time point of heme synthesis inhibition because this corresponded to the depleted regulatory heme pool, reflected by a 2-fold up-regulation of *ALAS1* and a relatively small (17%) reduction of total cellular heme.

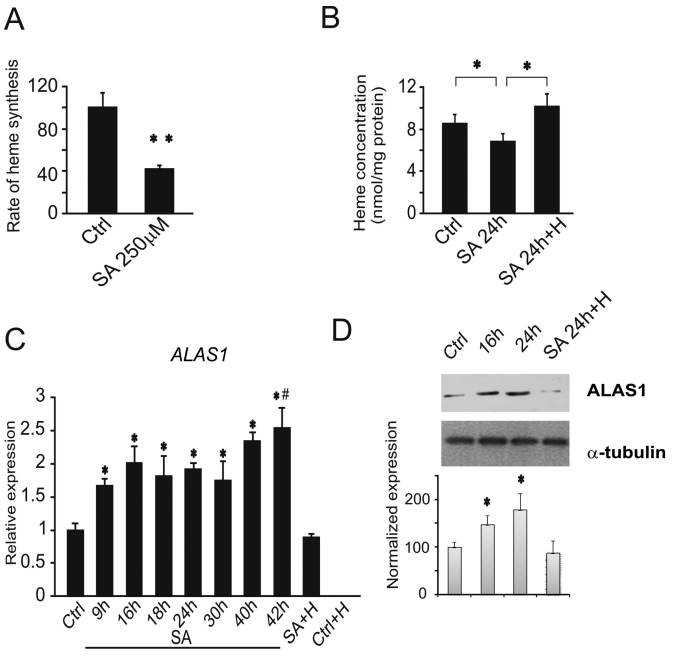

Fig. 1. Reduction of neuronal intracellular heme follows treatment with an inhibitor of heme synthesis, SA. Neurons maintained for 12 DIV were treated with 250 μM SA for 9 to 24 h with or without exogenous heme. A, rate of heme synthesis. Treated and control neurons were incubated with [3,5-^{3}H]aminolevulinic acid hydrochloride for 24 h on day 14, and then labeled heme was extracted and measured (n = 5), **, $p < 0.01$. B, concentration of intracellular heme in control, treated with SA and cotreated with SA and 0.1 μM heme (n = 5); *, statistically different, $p < 0.05$. C, up-regulation of *ALAS1* as a result of reduction of "free" heme in the cells occurs within hours after inhibition of heme synthesis. *ALAS1* expression measured by real-time PCR in control, SA-treated and cotreated with SA and 0.1 μM heme. Data denote mean ± S.D. of at least three independent experiments. *, statistically different from control group, $p < 0.05$; #, statistically different from 9-h time point. D, increase of ALAS1 protein in response to inhibition of heme synthesis for 16 and 24 h. Expression of ALAS1 in microsomal fraction in control and treated with SA neurons detected by Western blot (bottom) shows the quantification of immunoblotting with ALAS1 expression normalized against α-tubulin; data denote mean ± S.D. of at least three independent experiments.

Reduction of Intracellular Heme Decreases Tyrosine Phosphorylation of NR2B. Although continuously heme-deficient neurons have reduced expression of NMDAR subunits at the stage of neurite loss (Chernova et al., 2007), the initial changes after inhibition of heme synthesis do not involve down-regulation in gene or protein expression for NMDAR subunits NR1 and NR2B (Supplemental Fig. 1, A–D). NR2B is a major tyrosine-phosphorylated protein regulated by SFKs in the postsynaptic density (Moon et al., 1994) and is impaired in heme-deficient neurons (Chernova et al., 2007). To examine the early changes caused by reduced heme availability, we used immunoblotting and immunostaining to monitor NR2B phosphorylation at Tyr1336 and Tyr1252 in the presence or absence of SFKs inhibitor PP2 and heme in neurons treated with SA for 24 h, the time point at which the 2-fold up-regulation of *ALAS1* indicated a depletion of the regulatory heme pool (Fig. 2, A–N). Phosphorylation of NR2B at Tyr1336 and Tyr1252 was diminished in neurons by incubation with PP2 and was markedly lower in SA-treated compared with control cultures (Fig. 2, A and B). PP2 and SA treatments had additive effects on the reduction in Tyr1336 and Tyr1252 phosphorylation (Fig. 2, A and B). In cultures cotreated with SA and heme, phosphorylation of Tyr1336 and Tyr1252 was unaffected (Fig. 2, A and B). The rescue effect by exogenous heme was abolished if these cultures were concomitantly treated with PP2 (Fig. 2, A and B). The levels of NR2B protein phosphorylated at Tyr1336 and Tyr1252 were also examined by immunostaining of neuronal cultures under the same conditions (Fig. 2, C–N). Together, these data provide strong evidence that compromised availability of heme impairs NR2B subunit phosphorylation, and this is an early event in heme deficiency-induced neurodegeneration. This raises the question of whether the functional outputs of NMDARs are also affected at this early stage.

NMDAR Current Is Promptly Impaired by Reduction of Intracellular Heme. Phosphorylation of NMDAR regulates the channel kinetics and the Ca^{2+} permeability and membrane localization and trafficking (Cull-Candy and Leszkiewicz, 2004). After the finding of altered NR2B subunit phosphorylation after reduction of cellular heme, we examined how the NMDAR current was affected by changes

of heme concentration. Whole-cell patch-clamp recordings were made from single cortical neurons maintained in dissociated culture (12 DIV) and treated with SA for 24 h in the presence or absence of heme. Reduction of intracellular heme for 24 h decreased NMDA-mediated whole-cell currents compared with control cultures [Fig. 3A, top (Ctrl), versus top middle traces (24 h SA)]. Neurons cotreated with SA and heme for the same time exhibited larger responses to NMDA application [Fig. 3A, bottom middle traces (24 h SA + H)]. Incubation of control cultures with 100 nM heme for 24 h did not have an effect on NMDA-evoked whole-cell current [Fig. 3A, bottom traces (24 h + H)]. Data summarized in Fig. 3B show I/V curves for neurons under control conditions, heme treatment, SA treatment, and SA treatment in the presence of heme. NMDA-evoked currents at 40-mV holding potential were suppressed after SA treatment, and this effect was reversed by cotreatment with heme (Fig. 3C). The rescue effect of heme on NMDAR current was abolished in heme-deficient cultures cotreated with SFK inhibitor PP2 (Supplemental Fig. 2, A–C). The results suggest that the impairment of NMDAR function in neurons with reduced heme is associated with compromised phosphorylation of the regulatory NR2B subunit.

Ca^{2+} Influx through NMDARs Is Reduced in Neurons with Low Intracellular Heme Levels. Because NMDARs are highly Ca^{2+}-permeable (Viviani et al., 2006), we monitored changes in intracellular Ca^{2+} in response to NMDA application, as a further index of channel function. Cultures (12 DIV) were loaded with Fura 2-AM and imaged using a charge-coupled device camera; NMDA was pressure-applied onto control or SA-treated (24–44 h) cultures. The ratio of fluorescence at 340 and 380 nm excitation was used as a measure of intracellular Ca^{2+} ($[Ca^{2+}]_i$). Basal $[Ca^{2+}]_i$ did not change in SA-treated cultures (data not shown), whereas response to NMDA application was affected. SA-treated neurons showed diminished Ca^{2+} influx (Fig. 4A) in response to NMDA (Δ ratio calculated as peak ratio minus basal ratio). Peak Ca^{2+} responses were reduced at all time points of SA treatment (Fig. 4B). Heme readmission during 24 h of SA treatment recovered the peak Ca^{2+} responses to control levels (Fig. 4B). The data confirm that NMDAR function is affected within 24 h after inhibition of heme biosynthesis.

NMDAR-Dependent Production of cGMP Is Affected by Reduction of Intracellular Heme. Neuronal nitric-oxide synthase (nNOS) is activated by Ca^{2+} influx through NMDAR, leading to downstream production of cGMP after NO activation of soluble guanylate cyclase. Production of cGMP in response to NMDAR stimulation in cultures with low heme was significantly reduced by 22 ± 2% compared with control cultures (Fig. 4C). The response to NMDA was affected after 16 h of inhibition of heme synthesis, and as NMDAR function declined with longer SA treatment, so did cGMP production (by 38 ± 4% at 42 h after SA addition). These results provide further evidence of NMDAR functional impairment as an early change in the neurons with compromised availability of heme.

Heme Deficiency Reduces Dendritic Spine Number. Formation of dendritic spines by cortical neurons is closely associated with synaptic assemblies and plasticity, and increased intracellular Ca^{2+} via NMDAR induces the formation and remodelling of dendritic spines (Ethell and Pas-

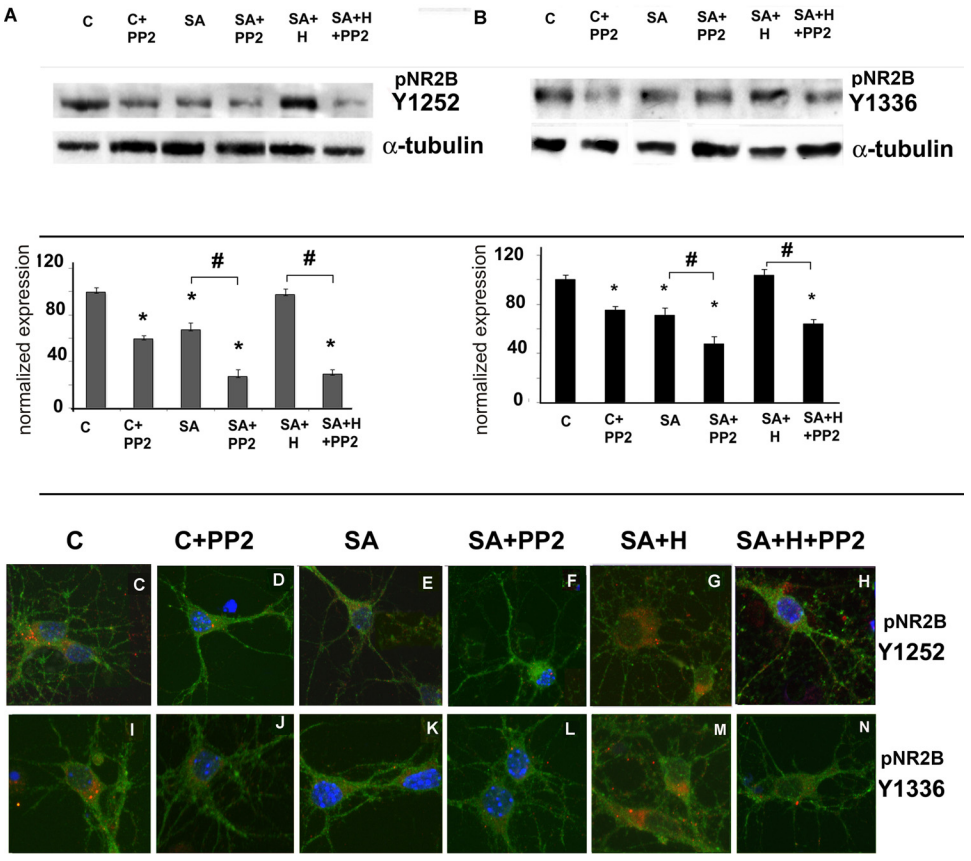

Fig. 2. Reduction of intracellular heme decreases NR2B tyrosine phosphorylation; exogenous heme reverses this change, and the rescue effect requires SFKs activity. Neurons were treated with 250 μM SA for 24 h with or without exogenous heme and with or without Src kinase inhibitor PP2 at 13 DIV. A, phosphorylation levels of NR2B at Tyr1252 and Tyr1336 corresponding to the above conditions were examined by Western blot; images show representative blots. The same blots were reprobed for α-tubulin. B, quantification of band intensities obtained using densitometry and ImageQuant 5.2 software and normalized to α-tubulin. Each column is the mean normalized expression of protein ± S.D. of at least three independent experiments. *, statistically different from control group, $p < 0.05$; #, statistically different, $p < 0.05$. C to N, confocal micrographs of maximum projection Z-series of cultured neurons at 13 DIV stained for phospho-NR2B (Tyr1252 and Tyr1336, top and bottom, respectively, red) and for PSD-95 (green), the nuclei were stained with 4′-6-diamidino-2-phenylindole (blue). C and I, control cultures; D and J, cultures treated with 50 nM PP2 for 2 h; E and K, SA treated for 18 h; F and L, treated with SA and PP2 for 18 h; G, H, M, and N, treated with SA and heme for 18 h in the presence (H and N) or absence (G and M) of PP2.

quale, 2005). Given the impaired NMDAR function we have observed in the neurons with reduced heme, we used imaging techniques to examine changes in dendritic spine formation. To visualize dendritic morphology, neurons were transfected with FLAG-tagged tdTomato (red fluorescent cell fill) at 7 DIV and then examined at 13 DIV after treatment with SA or SA and heme for 24 h with or without addition of the SFKs inhibitor PP2. Cortical neurons with pyramidal morphology were selected for analysis from the transfected cell population. The number of spines per 10 μM length of dendrite was significantly lower in the neurons with reduced cellular heme, whereas cotreatment of these cultures with heme reversed this phenomenon (Fig. 5, A–C, F). Inhibition of SFKs abolished the rescue effect of heme (Fig. 5,E and F) but did not cause further deterioration in spine formation in SA-treated cultures (Fig. 5, D and E). These findings suggest a mechanistic link between failure of NMDAR and spine formation at early stage of heme deficiency and provide evidence that the rescue by heme is NR2B phosphorylation-dependent.

Heme Modulates NMDAR Function and NR2B Phosphorylation within Minutes. To examine whether the potentiation of NMDA-mediated current by heme is a signaling event, we conducted whole-cell patch-clamp recordings simultaneously with reintroducing heme to the heme-deficient neurons and recorded for 13 min, after which currents reached plateau levels under all recording conditions (Fig. 6A). The neurons treated with SA for 24 h showed a 60% reduction in NMDA-evoked currents (Fig. 6A, blue diamonds) over a recording time of 13 min, which is consistent with a dialysis process and a current run down. Heme was introduced into the bath solution after 2 min of recording and caused a 40% increase in the NMDAR current (red square; after an initial 2-min decrease before heme addition). When heme was present in the patching pipette, there was no initial decrease, and the increase of the current started immediately (Fig. 6A, green triangles). At the 13-min time point, NMDA-evoked currents were ~140% of initial currents values if heme was added to the bath and ~110% if heme was present in the pipette. In contrast, in SA-treated cells currents, were only ~40% of initial values after 13 min of recording. Comparison of the three curves showed that by 10-min exposure to heme, the NMDAR current is 2- to 3-fold larger than in the absence of heme.

These alterations of the ion channel function correlated with the changes in NR2B phosphorylation levels upon readmission of heme to heme-deficient neurons (Fig. 6, B and C). At a 15-min time point, NR2B phosphorylation of NR2B at Tyr1252 and Tyr1336 were recovered to control levels. However, if these neurons were pretreated for 2 h with PP2, the rescue effect of heme was abolished, similar to the changes

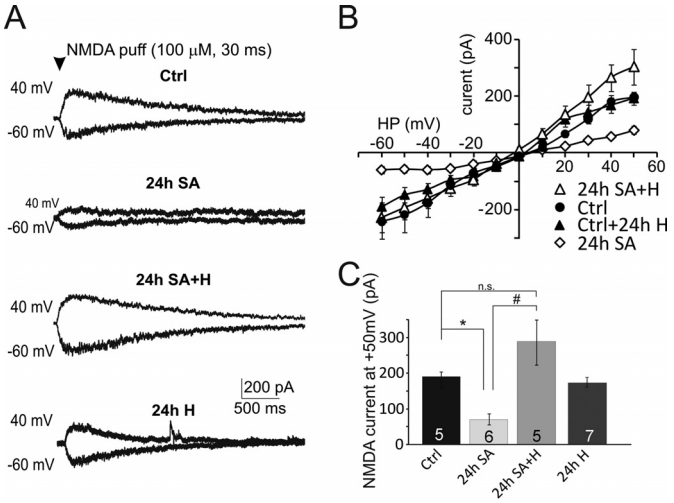

Fig. 3. Inhibition of heme synthesis promptly leads to suppression of NMDA-evoked currents; heme readmission reverses this change. A, whole-cell currents evoked by pressure application of NMDA (indicated by arrow; 100 μM, 20 p.s.i., 30 ms) to cortical neurons at holding potentials of −60 and +40 mV in control (top) and from neurons treated with SA for 24h (top middle), SA in the presence of heme (bottom middle), and control neurons treated with heme (bottom). B, I-V relationships for recorded NMDA currents under the same conditions. SA treatment reduced NMDA-evoked current over all voltages tested (SA) but not in the cells cotreated with heme. C, summary graph of NMDA currents at +40 mV holding potential under the three conditions. Data denote mean ± S.E.M. of at least five different cells (n shown in each bar). Significance assessed using analysis of variance; *, $p < 0.01$.

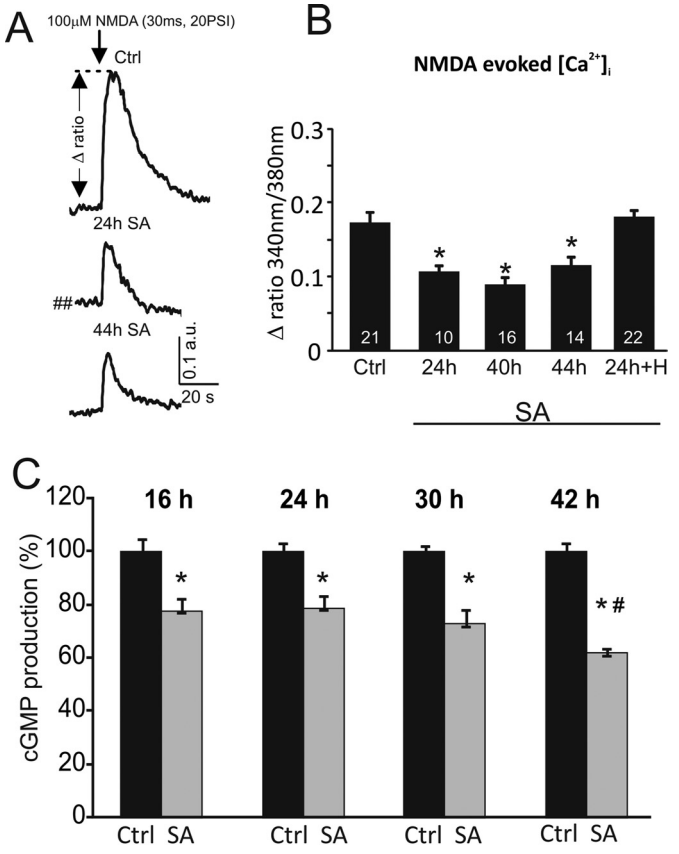

Fig. 4. Heme depletion reduces NMDA-evoked Ca^{2+} influx and Ca^{2+}-dependent cGMP production. The ratio of fluorescence at 340 and 380 nm excitation in the cell soma was used as a measure of $[Ca^{2+}]_i$. A, representative 340/380 nm ratio traces of NMDA-evoked intracellular Ca^{2+} ($[Ca^{2+}]_i$) in control cells (Ctrl) and in cells treated with SA for 24 and 44 h at 12 to 13 DIV. B, NMDA-evoked Ca^{2+} responses (Δratio, peak − basal) are reduced after 24 h of SA treatment but rescued by exogenous heme. Data denote mean ± S.E.M. of at least three cells from each of the three independent experiments (n shown in each bar). C, Ca^{2+}-dependent production of cGMP is decreased in neurons with reduced intracellular heme. Neurons (12–13 DIV) were treated with 250 μM SA and harvested after 16, 24, 30, or 42 h of treatment, cGMP production was monitored by radioimmunoassay, and measurements are expressed as the percentage of cGMP production in control cultures. Data denote the mean ± S.D. of three independent experiments. *, statistically different from control group, $p < 0.05$; #, statistically different from SA treatment for 16 h, $p < 0.05$.

observed in cultures cotreated with heme and SA for 24 h. These data show that regulation of NMDAR by heme is exerted rapidly and suggest a phosphorylation-dependent signaling mechanism.

Heme Is Preserved in Major Hemoproteins in Neurons Despite Depletion of Regulatory Pool. Depletion of heme from the regulatory pool clearly occurred within hours of SA treatment. We investigated what effect this treatment had on various hemoprotein functions in neurons.

Many mitochondrial proteins are hemoproteins, including those engaged in the electron transport chain and ATP generation. Mitochondrial membrane potential ($\Delta\Psi m$) and ATP generation were monitored after inhibition of heme synthesis to determine whether mitochondrial hemoproteins functions were affected in neurons when total cellular heme was reduced by ~17%. Inhibition of heme synthesis for at least 72 h had no effect on $\Delta\Psi m$ (Fig. 7, A and B), consistent with a well-sustained ATP generation in SA-treated neurons. Further measurement of ATP concentration (up to 6 days of heme synthesis inhibition) revealed that mitochondrial function was also unaffected in these cultures (Fig. 7C). These data show that heme was not depleted from mitochondrial hemoproteins under these conditions.

Soluble guanylate cyclase (sGC) is a hemoprotein which, on binding NO to heme, increases cGMP production up to 300-fold (Ballou et al., 2002). sGC activation by the NO donor *S*-nitroso-*N*-acetylpenicillamine was measured as the ratio of basal to stimulated cGMP accumulation and was similar in control cultures and those treated with SA for 42 h (Fig. 8A), demonstrating that the capacity of sGC to generate cGMP was unaffected.

The hemoprotein nNOS catalyzes the NADPH-dependent oxidation of L-arginine to citrulline and NO (White and Marletta, 1992). nNOS is a homodimer with heme as a prosthetic group controlling subunit dimerization and the quaternary structure of nNOS (Klatt et al., 1996). In contrast, heme-deficient enzyme (apo-nNOS) is an inactive monomer that degrades rapidly in vitro (Dunbar et al., 2004). The amount of

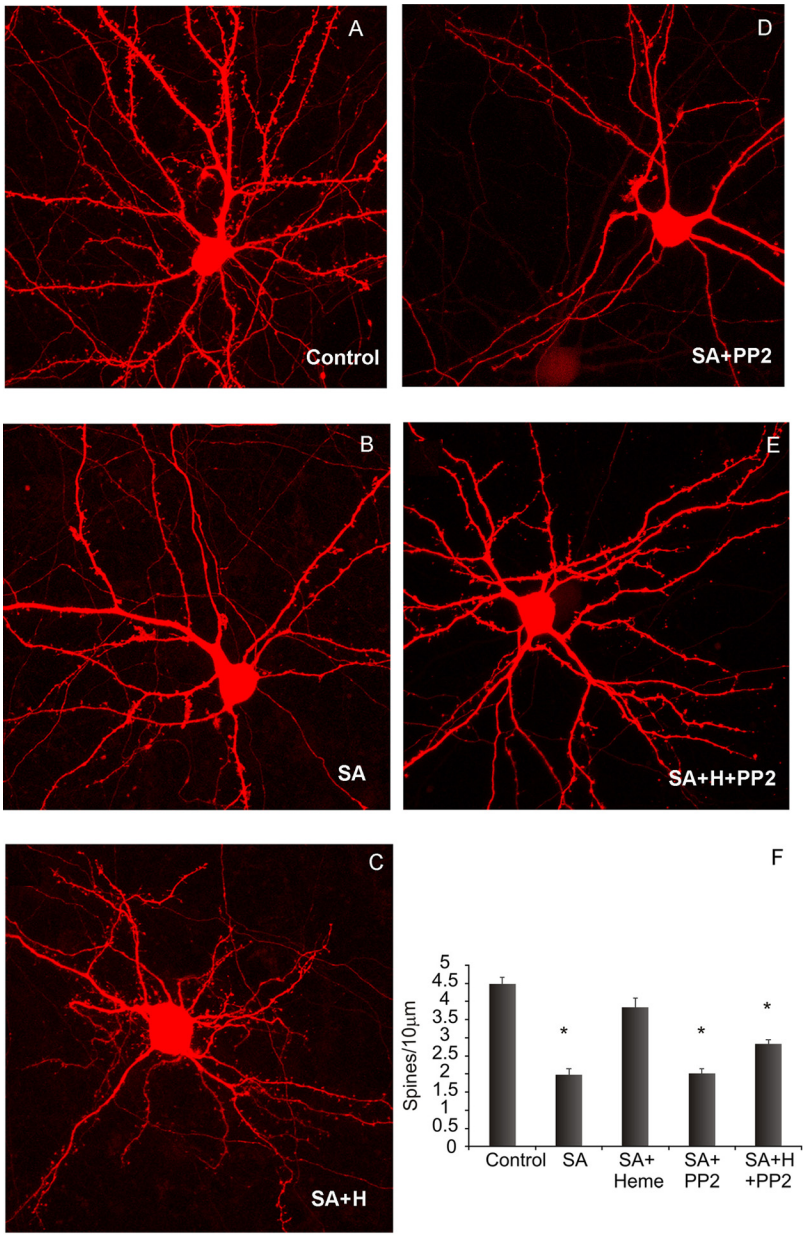

Fig. 5. Spine formation is reduced in neurons with deficient intracellular heme and rescued by exogenous heme; the rescue effect is NR2B phosphorylation-dependent. A to F, confocal micrographs of maximum projection Z-series of control (A), treated with SA (B) or SA and heme (C), SA and PP2 (D), and SA, heme, and PP2 (E) neurons transfected with FLAG-tagged tdTomato expressing red fluorescent cell-filling to visualize dendritic morphology. F, quantification of spines (number per length, $n = 16–25$) in cultures from three independent experiments; *, $p < 0.05$.

nNOS protein in neurons after 72 h inhibition of heme synthesis was similar in heme-depleted and control cultures (Fig. 8B), consistent with nNOS being in a stable and active homodimer in SA-treated cultures at 72 h.

HO-1 heme serves as both the substrate for the enzyme and the prosthetic group. The amount of HO-1 protein in the microsomal fraction of neuronal lysates was not reduced in the SA-treated neurons (Fig. 8C), suggesting that HO-1 basal expression was not affected when total cellular heme was decreased by ~17%.

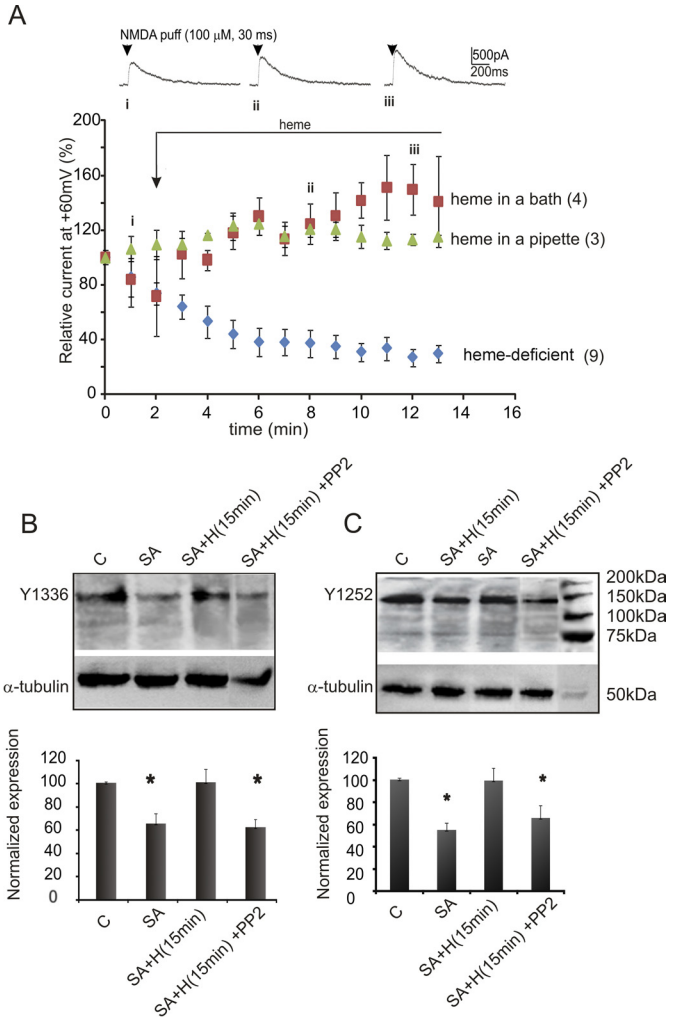

Fig. 6. Short-term effects of heme on function and phosphorylation of NMDAR. A, heme-deficient SA-treated (24 h) neurons ($n = 9$) showed a 70% reduction in NMDA-evoked currents (blue diamonds) over a recording time of 13 min. When heme (0.1 μM) was applied in the bath at 2 min (indicated by the arrow), the initial current decrease stopped, and NMDA-evoked currents were potentiated by 40% over 13 min (squares, $n = 4$). Top raw traces indicate representative currents at the indicated time points (i–iii). When heme was present in the patch pipette, currents started to increase immediately after patching (triangles, $n = 3$). B and C, exogenous heme rapidly restores phosphorylation of NR2B subunit at Tyr1252 and Tyr1336 in SA-treated neurons, inhibition of Src kinase abolishes the rescue effect of heme. Neurons at 13 DIV were treated with 250 μM SA for 24 h followed by 15-min incubation with exogenous heme with or without 2-h pretreatment with Src kinase inhibitor PP2. Phosphorylation levels of NR2B at Tyr1336 (B) and Tyr1252 (C) corresponding to the above conditions were examined by Western blot; images show representative blots. The same blots were reprobed for α-tubulin. Bottom, quantification of band intensities obtained using densitometry and ImageQuant 5.2 software and normalized to α-tubulin. Each column is the mean normalized expression of protein ± S.D. of three independent experiments. *, statistically different from control group, $p < 0.05$.

Cytochromes P450 (P450) are drug- and steroid-metabolizing enzymes expressed in various tissues, including brain. Two isoforms, CYP1A1 and CYP4X1(Al-Anizy et al., 2006), were detected in the microsomal fraction by immunoblotting (Fig. 8, D and E). No differences in protein expression were seen between control and SA-treated for 24 h cultures. Heme also is a positive modulator of P450 gene transcription, and low heme concentration may be a limiting factor for gene expression (Dwarki et al., 1987). We monitored *CYP4X4* gene expression in cultures with inhibited heme synthesis for up to 14 days and did not observe any down-regulation (Fig. 8F). Together, these data show that heme bound in mitochondrial and others major hemoproteins, such as sGC, nNOS, CYP1a1 and CYP4X1, remained in this state associated with proteins after reduction of heme synthesis by ~50% and depletion of the regulatory heme pool.

Discussion

We showed previously that heme deficiency in primary neurons causes neuronal degeneration (Chernova et al., 2007); however, the mechanisms triggering neuronal damage are not well understood. Here, we explored the mechanisms by which a deficit of heme affects synaptic function at an early stage of neurodegeneration, before neurite fragmentation in primary neurons. We have shown early loss of NMDAR function, which correlated with reduced phosphorylation of NR2B subunits. Reduced NMDAR currents and Ca^{2+} influx affected NMDAR-dependent cGMP production and were accompanied by deficient formation of dendritic spines. In this study, we used selective and specific inhibition of the second enzyme aminolevulinic acid dehydratase in the heme synthetic pathway, which remains the optimal means

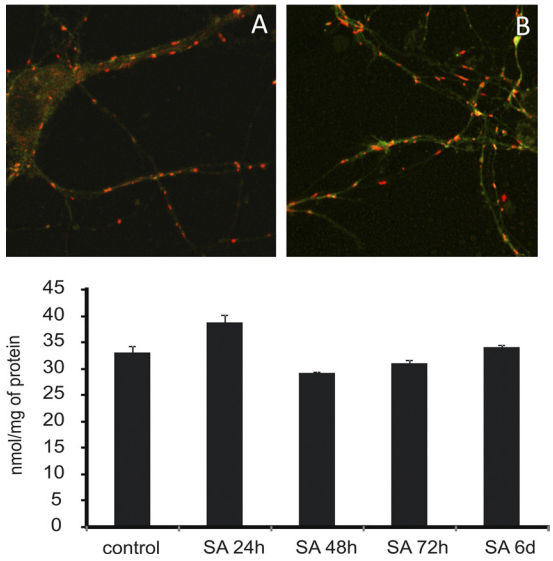

Fig. 7. Mitochondrial membrane potential was unaffected in neurons with moderately reduced intracellular heme. Control (A) and neurons treated with 250 μM SA for 72 h (B) were stained with 5,5′,6,6′-tetrachloro-1,1′,3,3′-tetraethylbenzimidazoyl carbocyanine iodide (DePsipher Kit) and displayed aggregation of the DePsipher within the mitochondria with high ΔΨm (red). C, ATP production in control and treated cultures with 250 μM SA up to 6 days measured by CellTiter-Glo Luminescent Cell Viability Assay. All measurements were conducted in triplicate, and ATP concentrations were normalized to total protein content in the samples. Error bars indicate the standard deviation of three samples with the same treatment from at least three independent experiments.

of modulating intracellular heme in vivo and in vitro (Zhu et al., 2002). ALAS1 is the first and rate-limiting enzyme, and consistent with depletion of the regulatory heme pool, we monitored the increased expression of this gene (Sassa and Nagai, 1996) and protein (Zheng et al., 2008), which is the generally accepted approach to reflect "free" heme levels (Raghuram et al., 2007). In our model, the rate of heme synthesis was reduced by ~50%, whereas total intracellular heme was reduced by ~17%, suggesting strong homeostatic mechanisms and supporting previous studies of heme turnover and transport (Maines and Gibbs, 2005). However, the reduction of heme cannot be attributed to reduction of the regulatory pool alone, which has been estimated as <100 nM (Sassa and Nagai, 1996). This decrease could be explained by the depletion of the regulatory pool and heme from cellular storage. Such heme storage was demonstrated in astrocytes and involved a reputed heme transporter HCP1 (Dang et al., 2010). It is plausible that core functions using cofactor heme (e.g., respiratory chain in mitochondrial cytochromes) would be protected by homeostatic mechanisms.

The dynamics of heme depletion in neurons were reflected by apparent reduction of regulatory heme within hours, whereas heme bound in hemoproteins remained at sufficient levels. Mitochondrial hemoproteins were not affected in the neurons with impaired synthesis, and mitochondrial function was not compromised for up to 6 days. This is consistent with the fact that the dissociation constant of mitochondrial hemoprotein heme is $<10^{-13}$ M, and "free" heme concentration is estimated at 10^{-7} M (Sassa, 2004). Therefore, "free" heme could be lowered by several orders of magnitude before the depletion of bound heme occurred. Furthermore, heme is covalently bound in some hemoproteins, and depletion would probably only occur with turnover of the protein. Heme was not depleted from sGC because cGMP production did not change when Ca^{2+}-dependent part of the pathway was bypassed. nNOS protein amounts were unaltered in SA-treated cultures, indicating sufficient heme levels to form nNOS homodimers and prevent protein degradation. The amounts of CYP1A1 and CYP4X1 proteins in microsomal fraction remained similar in control and treated cells. Impaired heme levels are believed to decrease CYP450 function via incomplete saturation of apoprotein (Jover et al., 2000), cytosolic

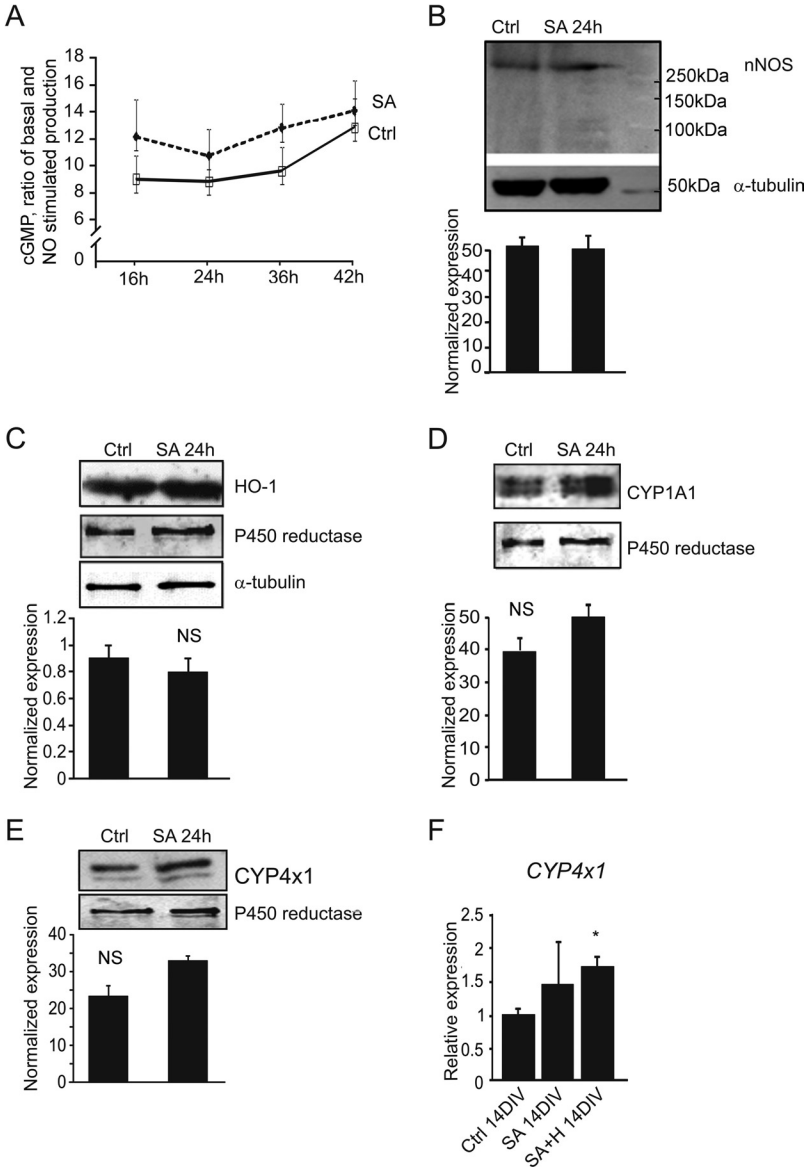

Fig. 8. Hemoprotein heme is preserved in neurons after reduction of heme synthesis. A), cGMP production in the presence of NO donor is maintained in heme-deficient neurons. Concentrations of cGMP in the control and SA-treated cultures were monitored in radioimmunoassay and expressed as fold stimulation in response to NO donor *S*-nitroso-*N*-acetylpenicillamine (the ratio of basal and NO-stimulated cGMP production). Data denote the mean ± S.D. of at least three independent experiments. B, expression of nNOS in control and treated neurons, whole-cell lysates were separated by native polyacrylamide gel electrophoresis and analyzed by immunoblotting. Bottom, quantification of nNOS band intensities normalized to α-tubulin, each column is the mean of normalized protein expression ± S.D. of three independent experiments. C, expression of HO-1 in microsomal fraction in control and neurons treated with SA detected by Western blot; bottom, quantification of immunoblotting with HO-1 expression normalized against microsomal protein P450 reductase; α-tubulin was detected in whole-cell lysate before isolation of microsomal fraction. Data denote mean ± S.D. of at least three independent experiments. D and E, expression of CYP4X1 and CYP1A1 in microsomal fraction of neurons treated with SA for 24 h compared with control. Bottom, quantification of Western blots, and expression levels are normalized to microsomal protein P450 reductase. Each column is the mean of normalized protein expression ± S.D. of three independent experiments. F, expression of CYP4X1 gene in control, heme-deficient neurons continuously treated with SA (2–14 DIV) and neurons treated with SA and heme for 12 days (2–14 DIV) measured by real-time PCR; β-actin was used as an endogenous reference gene.

persistence of the protein (Meyer et al., 2005), and involvement of heme in transcriptional regulation (Dwarki et al., 1987). Our data did not contradict these suggestions but indicated that more time is required to develop heme deficiency in these functional compartments.

In contrast to hemoproteins, the regulatory pool of heme was depleted promptly after starting treatment and resulted in NMDAR dysfunction. After 24 h of SA treatment, NMDA-evoked current was decreased by more than 50%, similar to the reduction monitored in the continuous model after 12 days of inhibition. This reduction cannot be related to a direct effect of SA on the receptor because in the presence of heme, SA-treated neurons showed a large response to NMDA, similar to control. High permeability of NMDAR for Ca^{2+} places the receptor in the upstream part of various signaling pathways. Physiological levels of synaptic NMDA receptor activation promote the survival of many types of neurons and increase their resistance to cellular damage (Hardingham and Bading, 2003). A marked decrease of Ca^{2+} influx in response to NMDA also reflects receptor dysfunction after reduction of heme and is consistent with diminished current. Ca^{2+} can enter cells through many pathways, including neurotransmitter-gated ion channels (NMDAR), Ca^{2+}-permeable subtypes of AMPA receptors, and voltage-dependent Ca^{2+} channels. There was no reduction in basal Ca^{2+} concentration in treated cells that can be attributed to compensatory Ca^{2+} flow through other receptors, whereas stimulation of NMDAR failed to produce an adequate response. The more sensitive radioimmunoassay of cGMP production detected reduction of NMDAR function even earlier. NMDAR-dependent cGMP production declined as inhibition of heme synthesis continued, suggesting that reduced cGMP concentration itself could contribute to the development of neurodegeneration in the continuous model. However, NMDAR functional failure was an earlier change in neurons with depleted regulatory heme and may have triggered alterations of many Ca^{2+}-dependent signaling pathways.

NMDARs play an important role in dendritic spine formation and maintenance. Elongation of existing spines and formation of new filopodia can be blocked by NMDAR antagonists (Shi et al., 2005). Decrease in Ca^{2+} influx affects the organization of cytoskeleton, trafficking of postsynaptic density (PSD) components, and recycling of proteins (Nimchinsky et al., 2002), thereby affecting spine formation. Reduction of spines after inhibition of heme synthesis could be another consequence of NMDR dysfunction. NR2B phosphorylation-dependent recovery of spine formation by heme indicates that NMDAR failure causes spine-formation deficit; however, we cannot exclude the interactions of heme with other proteins. Ca^{2+} current through the NMDAR is largely regulated by its NR2B subunit (Krapivinsky et al., 2003), and tyrosine phosphorylation of NR2B is essential to sustain the elevation of neuronal Ca^{2+} current (Viviani et al., 2006). We have shown that a marked decrease in NR2B tyrosine phosphorylation was an early change after the reduction of regulatory heme in neurons. Similar to NMDA-evoked current, NR2B phosphorylation was rescued by exogenous heme, suggesting a coupling of these recovery mechanisms. Inhibition of SFKs abolished the rescue effect of heme on NMDAR currents, providing further evidence of the mechanistic link. Replenishment of heme concentration could reverse early synaptic changes, but only if NR2B phosphorylation was resumed. This and additive effects of PP2 and SA on NR2B phosphorylation suggest that heme is involved in maintaining NMDAR function via its phosphorylation. Heme modulates NMDAR function in an acute signaling mode, suggesting a direct interaction, probably within the NMDAR complex and with involvement of SFKs. Exogenous heme alters phosphorylation status of tyrosine kinases in heme-deficient cells (Yao et al., 2010). Src and Jak2 phosphorylations (Tyr530 and Tyr1007, respectively) were increased by heme, and the first has an inhibitory effect on activity of Src, and the latter activates JAK2. NR2B phosphorylation at Tyr1252 and Tyr1336 monitored in our study is regulated by Fyn member of SFKs (Nakazawa et al., 2001). There is an evidence of JAK2 cross-talk with SFKs (Jiang et al., 2008); however, it requires further clarification of how heme, JAK2, and NMDAR may interact. It is noteworthy that a mitochondrial protein NADH dehydrogenase subunit 2 was found recently to act as an adapter protein anchoring Src to the NMDAR, thereby playing a crucial role for Src regulation of synaptic NMDAR activity. NADH dehydrogenase subunit 2 is a subunit of complex I in mitochondria, but in the brain, it interacts with Src outside of this organelle (Gingrich et al., 2004). Using hemin-agarose affinity chromatography of neuronal lysates followed by proteomics analysis, we identified a number of putative heme-binding proteins, including partners of NMDAR complex and constituents of mitochondrial complexes I and II, which can be potential sites for regulation (Supplemental Table 1). Heme binding resulting in conformational changes of a target protein (e.g., a kinase or a protein facilitating a phosphorylation) is a plausible mechanism of the rapid increase of NMDAR currents by heme. Further systematic examination is required to identify exact targets of heme interactions with synaptic proteins.

Subunit-specific phosphorylation also controls differentially the trafficking and surface expression of NMDARs (Cull-Candy and Leszkiewicz, 2004), and monitoring these phosphorylations in heme-deficient neurons will be addressed in future studies aimed of the relationships in the NMDAR complex in heme-deficiency induced neurodegeneration. The alterations in NMDAR signaling seen in heme-depleted neurons could be the trigger for neurite decay. Functional and molecular connections of NMDARs with other receptors, such as AMPA and metabotropic glutamate receptors, are very complex, and at this stage, we cannot exclude contributions from other receptors and synaptic proteins to neuronal decay in heme-deficient cultures. However, rapid and reversible changes in NMDAR function and in phosphorylation of its regulatory subunit correlated with the availability of heme couple the receptor and heme in a signaling mode.

Together, these findings lead to the conclusion that depletion of regulatory heme rapidly compromises NR2B phosphorylation and causes the dysfunction of NMDARs; this compromises calcium-dependent signaling pathways and triggers changes in cGMP production and dendritic spine formation. Synaptic changes precede the depletion of heme from major hemoproteins. Further exploration of heme interaction with NMDAR complex and understanding how exactly the effects of heme are exerted and could be modulated by drugs may provide new insights into the reversal of neurodegeneration.

Acknowledgments

We thank the members of the University of Leicester Biomedical Services staff for their assistance; Dr. Michael J. Schell (Department of Pharmacology, Uniformed Services University, Bethesda, MD) for the gift of FLAG-tagged tdTomato construct; and Dr. D. Bell (School of Biology, University of Nottingham, Nottingham, UK) for the gift of CYP4X1 antibody.

Authorship Contributions

Participated in research design: Chernova, Smith, and Forsythe.
Conducted experiments: Chernova, Steinert, Richards, and Mistry.
Contributed new reagents or analytic tools: Jukes-Jones and Cain.
Wrote or contributed to the writing of the manuscript: Chernova, Steinert, Smith, and Forsythe.

References

Al-Anizy M, Horley NJ, Kuo CW, Gillett LC, Laughton CA, Kendall D, Barrett DA, Parker T, and Bell DR (2006) Cytochrome P450 Cyp4x1 is a major P450 protein in mouse brain. *FEBS J* **273:**936–947.
Atamna H and Frey WH, 2nd (2004) A role for heme in Alzheimer's disease: heme binds amyloid beta and has altered metabolism. *Proc Natl Acad Sci USA* **101:** 11153–11158.
Ballou DP, Zhao Y, Brandish PE, and Marletta MA (2002) Revisiting the kinetics of nitric oxide (NO) binding to soluble guanylate cyclase: the simple NO-binding model is incorrect. *Proc Natl Acad Sci USA* **99:**12097–12101.
Boekhoorn K, Terwel D, Biemans B, Borghgraef P, Wiegert O, Ramakers GJ, de Vos K, Krugers H, Tomiyama T, Mori H, Joels M, van Leuven F, and Lucassen PJ (2006) Improved long-term potentiation and memory in young tau-P301L transgenic mice before onset of hyperphosphorylation and tauopathy. *J Neurosci* **26:** 3514–3523.
Brooker G, Harper JF, Terasaki WL, and Moylan RD (1979) Radioimmunoassay of cyclic AMP and cyclic GMP. *Adv Cyclic Nucleotide Res* **10:**1–33.
Chernova T, Nicotera P, and Smith AG (2006) Heme deficiency is associated with senescence and causes suppression of N-methyl-D-aspartate receptor subunits expression in primary cortical neurons. *Mol Pharmacol* **69:**697–705.
Chernova T, Steinert JR, Guerin CJ, Nicotera P, Forsythe ID, and Smith AG (2007) Neurite degeneration induced by heme deficiency mediated via inhibition of NMDA receptor-dependent extracellular signal-regulated kinase 1/2 activation. *J Neurosci* **27:**8475–8485.
Cull-Candy SG and Leszkiewicz DN (2004) Role of distinct NMDA receptor subtypes at central synapses. *Sci STKE* **2004:**re16.
Dang TN, Bishop GM, Dringen R, and Robinson SR (2010) The putative heme transporter HCP1 is expressed in cultured astrocytes and contributes to the uptake of hemin. *Glia* **58:**55–65.
Dunbar AY, Kamada Y, Jenkins GJ, Lowe ER, Billecke SS, and Osawa Y (2004) Ubiquitination and degradation of neuronal nitric-oxide synthase in vitro: dimer stabilization protects the enzyme from proteolysis. *Mol Pharmacol* **66:**964–969.
Dwarki VJ, Francis VN, Bhat GJ, and Padmanaban G (1987) Regulation of cytochrome P-450 messenger RNA and apoprotein levels by heme. *J Biol Chem* **262:**16958–16962.
Ethell IM and Pasquale EB (2005) Molecular mechanisms of dendritic spine development and remodeling. *Prog Neurobiol* **75:**161–205.
Gingrich JR, Pelkey KA, Fam SR, Huang Y, Petralia RS, Wenthold RJ, and Salter MW (2004) Unique domain anchoring of Src to synaptic NMDA receptors via the mitochondrial protein NADH dehydrogenase subunit 2. *Proc Natl Acad Sci USA* **101:**6237–6242.
Hardingham GE and Bading H (2003) The Yin and Yang of NMDA receptor signalling. *Trends Neurosci* **26:**81–89.
Ishii DN and Maniatis GM (1978) Haemin promotes rapid neurite outgrowth in cultured mouse neuroblastoma cells. *Nature* **274:**372–374.
Jiang L, Li Z, and Rui L (2008) Leptin stimulates both JAK2-dependent and JAK2-independent signaling pathways. *J Biol Chem* **283:**28066–28073.
Jover R, Hoffmann F, Scheffler-Koch V, and Lindberg RL (2000) Limited heme synthesis in porphobilinogen deaminase-deficient mice impairs transcriptional activation of specific cytochrome P450 genes by phenobarbital. *Eur J Biochem* **267:**7128–7137.
Kannan M, Steinert JR, Forsythe ID, Smith AG, and Chernova T (2010) Mevastatin accelerates loss of synaptic proteins and neurite degeneration in aging cortical neurons in a heme-independent manner. *Neurobiol Aging* **31:**1543–1553.
Kapoor N, Pant AB, Dhawan A, Dwievedi UN, Gupta YK, Seth PK, and Parmar D (2006) Differences in sensitivity of cultured rat brain neuronal and glial cytochrome P450 2E1 to ethanol. *Life Sci* **79:**1514–1522.
Klatt P, Pfeiffer S, List BM, Lehner D, Glatter O, Bächinger HP, Werner ER, Schmidt K, and Mayer B (1996) Characterization of heme-deficient neuronal nitric-oxide synthase reveals a role for heme in subunit dimerization and binding of the amino acid substrate and tetrahydrobiopterin. *J Biol Chem* **271:**7336–7342.
Krapivinsky G, Krapivinsky L, Manasian Y, Ivanov A, Tyzio R, Pellegrino C, Ben-Ari Y, Clapham DE, and Medina I (2003) The NMDA receptor is coupled to the ERK pathway by a direct interaction between NR2B and RasGRF1. *Neuron* **40:**775–784.
Maines MD and Gibbs PE (2005) 30 some years of heme oxygenase: from a "molecular wrecking ball" to a "mesmerizing" trigger of cellular events. *Biochem Biophys Res Commun* **338:**568–577.
Mallucci GR (2009) Prion neurodegeneration: starts and stops at the synapse. *Prion* **3:**195–201.
Meyer RP, Lindberg RL, Hoffmann F, and Meyer UA (2005) Cytosolic persistence of mouse brain CYP1A1 in chronic heme deficiency. *Biol Chem* **386:**1157–1164.
Moon IS, Apperson ML, and Kennedy MB (1994) The major tyrosine-phosphorylated protein in the postsynaptic density fraction is N-methyl-D-aspartate receptor subunit 2B. *Proc Natl Acad Sci USA* **91:**3954–3958.
Nakazawa T, Komai S, Tezuka T, Hisatsune C, Umemori H, Semba K, Mishina M, Manabe T, and Yamamoto T (2001) Characterization of Fyn-mediated tyrosine phosphorylation sites on GluR epsilon 2 (NR2B) subunit of the N-methyl-D-aspartate receptor. *J Biol Chem* **276:**693–699.
Nimchinsky EA, Sabatini BL, and Svoboda K (2002) Structure and function of dendritic spines. *Annu Rev Physiol* **64:**313–353.
Ogawa K, Sun J, Taketani S, Nakajima O, Nishitani C, Sassa S, Hayashi N, Yamamoto M, Shibahara S, Fujita H, and Igarashi K (2001) Heme mediates derepression of Maf recognition element through direct binding to transcription repressor Bach1. *EMBO J* **20:**2835–2843.
Raghuram S, Stayrook KR, Huang P, Rogers PM, Nosie AK, McClure DB, Burris LL, Khorasanizadeh S, Burris TP, and Rastinejad F (2007) Identification of heme as the ligand for the orphan nuclear receptors REV-ERBalpha and REV-ERBbeta. *Nat Struct Mol Biol* **14:**1207–1213.
Sassa S (2004) Why heme needs to be degraded to iron, biliverdin IXalpha, and carbon monoxide? *Antioxid Redox Signal* **6:**819–824.
Sassa S and Nagai T (1996) The role of heme in gene expression. *Int J Hematol* **63:**167–178.
Shi GX, Han J, and Andres DA (2005) Rin GTPase couples nerve growth factor signaling to p38 and b-Raf/ERK pathways to promote neuronal differentiation. *J Biol Chem* **280:**37599–37609.
Shinjyo N and Kita K (2006) Up-regulation of heme biosynthesis during differentiation of Neuro2a cells. *J Biochem* **139:**373–381.
Soto C and Estrada LD (2008) Protein misfolding and neurodegeneration. *Arch Neurol* **65:**184–189.
Tang XD, Xu R, Reynolds MF, Garcia ML, Heinemann SH, and Hoshi T (2003) Haem can bind to and inhibit mammalian calcium-dependent Slo1 BK channels. *Nature* **425:**531–535.
Viviani B, Gardoni F, Bartesaghi S, Corsini E, Facchi A, Galli CL, Di Luca M, and Marinovich M (2006) Interleukin-1 beta released by gp120 drives neural death through tyrosine phosphorylation and trafficking of NMDA receptors. *J Biol Chem* **281:**30212–30222.
White KA and Marletta MA (1992) Nitric oxide synthase is a cytochrome P-450 type hemoprotein. *Biochemistry* **31:**6627–6631.
Wishart TM, Parson SH, and Gillingwater TH (2006) Synaptic vulnerability in neurodegenerative disease. *J Neuropathol Exp Neurol* **65:**733–739.
Yao X, Balamurugan P, Arvey A, Leslie C, and Zhang L (2010) Heme controls the regulation of protein tyrosine kinases Jak2 and Src. *Biochem Biophys Res Commun* **403:**30–35.
Zheng J, Shan Y, Lambrecht RW, Donohue SE, and Bonkovsky HL (2008) Differential regulation of human ALAS1 mRNA and protein levels by heme and cobalt protoporphyrin. *Mol Cell Biochem* **319:**153–161.
Zhu Y, Hon T, Ye W, and Zhang L (2002) Heme deficiency interferes with the Ras-mitogen-activated protein kinase signaling pathway and expression of a subset of neuronal genes. *Cell Growth Differ* **13:**431–439.

Address correspondence to: Dr. Tatyana Chernova, MRC Toxicology Unit, Hodgkin Building, University of Leicester, Lancaster Road, Leicester, LE1 9HN. E-mail: tc28@le.ac.uk